

Temporal dynamics of flooding, evaporation, and desiccation cycles and observations of salt crust area change at the Bonneville Salt Flats, Utah



Brenda B. Bowen^{a,b,*}, Evan L. Kipnis^a, Logan W. Raming^a

^a Department of Geology and Geophysics, University of Utah, 115 South 1460 East, Frederic A. Sutton Building 205, Salt Lake City, UT 84112, USA

^b Global Change and Sustainability Center, University of Utah, Salt Lake City, UT 84112, USA

ARTICLE INFO

Article history:

Received 1 June 2017

Received in revised form 28 September 2017

Accepted 28 September 2017

Available online 02 October 2017

Keywords:

Bonneville Salt Flats

Playa

Halite

Surface processes

Evaporite basins

ABSTRACT

The Bonneville Salt Flats (BSF) in Utah is a dynamic saline playa environment responding to natural and anthropogenic forces. Over the last century, the saline groundwater from below BSF has been harvested to produce potash via evaporative mining, mostly used as agricultural fertilizers, while the surface halite crust has provided a significant recreational site for land speed racing. Perceptions of changes in the salt crust through time have spurred debates about land use and management; however, little is known about the timescales of natural change as the salt crust responds to climatic parameters that drive flooding, evaporation, and desiccation (FED) cycles that control surface salt growth and dissolution. Climate data over the last ~30 years are examined to identify annual patterns in surface water balance at BSF to identify annual and seasonal climate constraints on FED cycles. Landsat satellite data from 1986 to the present are used to map the areal extent of the surface halite salt crust at BSF at the end of the desiccation season (between August 15 and October 30) annually. Overall, the observed area of the desiccation-stage BSF halite crust has varied from a maximum of 156 km² in 1993 to a minimum of 72 km² in 2014 with an overall trend of declining area of halite observed over the ~30 years of analysis. Climatic variables that influence FED cycles and seasonal salt dissolution and precipitation have also varied through this time period; however, the relationship between surface water fluxes and salt crust area do not clearly correlate, suggesting that other processes are influencing the extent of the salt. Intra-annual analyses of salt area and weather illustrate the importance of ponded surface water, wind events, and microtopography in shaping a laterally extensive but thin and ephemeral halite crust. Examination of annual to decadal changes in salt crust extent and environmental parameters at BSF provides insights into the processes driving change and the sustainability of land use in this dynamic environment.

© 2017 Elsevier B.V. All rights reserved.

1. Introduction

The Bonneville Salt Flats (BSF) are located in the western end of the Great Salt Lake Desert (GSLD), Utah, and are a part of the larger Bonneville basin playa system defined by its closed surface hydrology as well as geomorphic and sedimentary surface remnants of Pleistocene Lake Bonneville (Fig. 1) (Turk, 1973; Oviatt, 2015). Near the state line between Utah and Nevada, an oval-shaped accumulation of surface efflorescent halite (NaCl) precipitates most summers from a seasonal standing brine pond along the western edge of the GSLD. The presence of this surface halite salt crust defines BSF, but the boundaries between BSF and the surrounding mudflats are transitional and change through time. This unique accumulation of saline minerals has fostered significant recreational and mining activities over the past century, resulting in a complex coupled system of human and natural interactions influencing the surface processes, hydrology, and changes in the

landscape. The role of anthropogenic processes in driving changes in the salt and specific physical, chemical, and biological processes leading to evaporite growth and dissolution over seasonal, annual, and decadal timescales at BSF are unclear but important to understand in order to inform sustainable management of this ephemeral and valued landscape.

The prevailing paradigm for the episodic formation and dissolution of surface saline minerals in continental evaporite basins follows cycles of flooding, evaporation, and desiccation (FED) of the playa surface (Lowenstein and Hardie, 1985). The FED cycles are generally defined by the surface water balance, chemistry of surface brines, and evaporite sediment deposition and dissolution. The timing of FED cycles can range from single storm events to intra-annual, seasonal, or decadal scales depending on local setting, hydrology, and climate. While some saline pans may be ephemeral, others can last for millennia if the hydrology and solute transport remain in a balance that promotes solute concentration, net water loss, and mineral accumulation (Warren, 2016).

During FED cycles, the flooding stage is characterized by the presence of a shallow, brackish surface pond. At BSF, an annual shallow (<60 cm) saline (~20–30% total dissolved solids) pond covers much of the surface from ~October through ~May (Fig. 2). This surface lake

* Corresponding author at: Department of Geology and Geophysics, University of Utah, 115 South 1460 East, Frederic A. Sutton Building 205, Salt Lake City, UT 84112, USA.

E-mail address: brenda.bowen@utah.edu (B.B. Bowen).

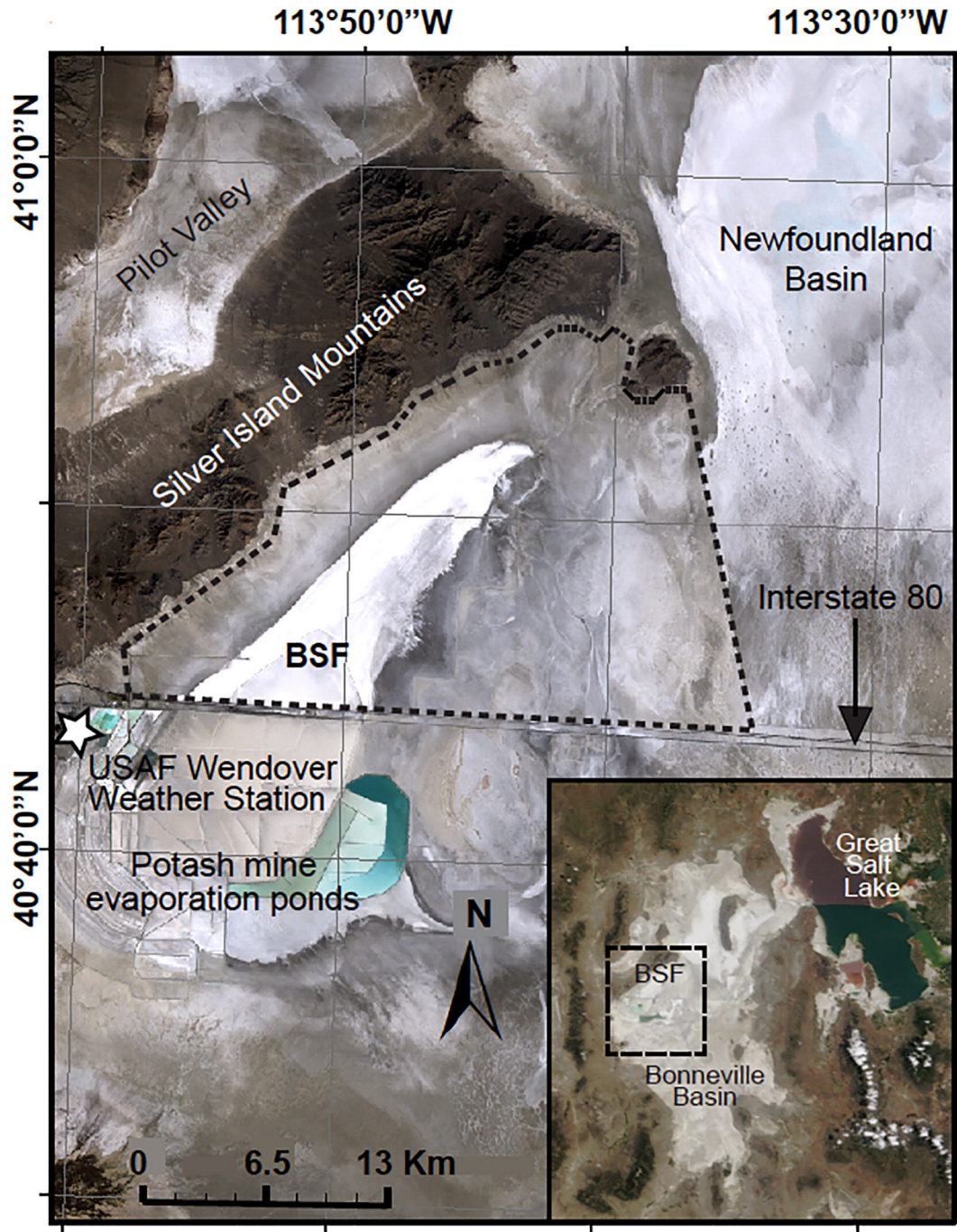


Fig. 1. Location of BSF in western Utah. Dashed line indicates extent of area analyzed with Landsat. Evaporation ponds are located on the south side of Interstate 80. Star indicates location of Air Force auxiliary field weather station. Inset box shows location of BSF within the context of the Bonneville basin and the Great Salt Lake.

water commonly is a combination of meteoric water that falls directly onto the surface and perched shallow saline groundwater (Benison et al., 2007; Bowen and Benison, 2009). Undersaturated surface water dissolves halite and increases the salinity of the brine. Standing water can also become quite turbid with input of mud, carbonate, and clay from the playa margins (Fig. 2A). With increasing evaporation and decreasing rainfall into the summer months, the surface brine evapoconcentrates, and halite crystals begin to form at the air-water interface (Fig. 2B). Halite *hoppers* crystalize on the brine surface forming rafts that eventually become heavy enough to sink through the brine and accumulate in layers on the playa floor. These halite crystals bury detrital sediments that have accumulated in the seasonal pond. Further into the evaporative cycles surface brine disappears and desiccation

continues through capillary evaporation of the shallow saline groundwater (Fig. 2C and D).

During most late summers, the hard, seasonally repaved halite surface, level ground, consistent texture, moisture content, and extensive area of BSF provide an ideal playground for speed enthusiasts; and land speed records have been set by many different classes of vehicles over the last century (Noeth, 2002). The high albedo of the bright salt maintains cool temperatures that keep tires, sometimes exceeding 600 mph, from overheating. The historically vast extent of the salt crust has provided the distance needed for racers to speed up and slow down safely. A passionate racing community with a strong connection to the salt crust and vested interested in the reliability and sustainability of this landscape has developed over the last century. In addition,

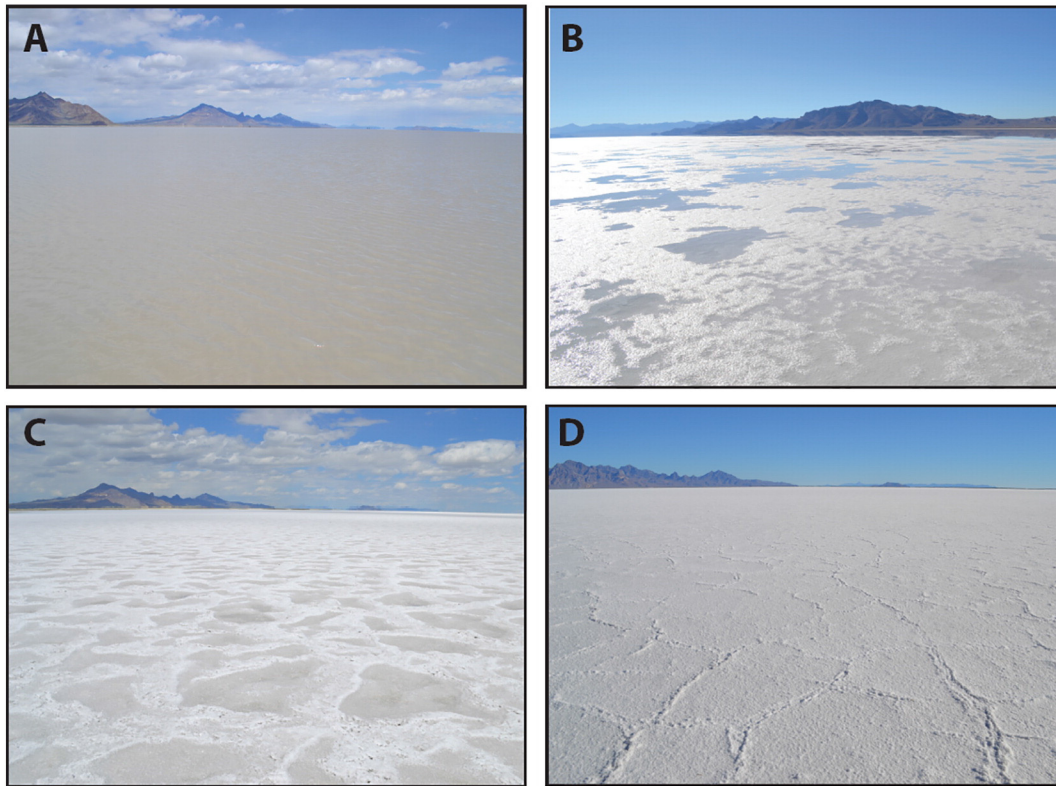


Fig. 2. Field photos of BSF during flooding (A), evaporation (B), and desiccation (C, D) stages. Note the turbidity in (A) because of the mud/clay from eolian input and entrainment of clay-rich playa sediments. In (B), halite rafts are forming at the water-air interface. These rafts eventually sink, are blown across the surface, and accumulate against pressure ridges as the shallow surface water evaporates (C). During desiccation, capillary evaporation through pore spaces creates additional efflorescent halite crust with polygonal ridges (D).

the regional shallow brine aquifer associated with the extensive halite crust provides a rich source of potassium accessible through evaporative mining, and various commercial mining operations have extracted saline resources from the environment over the past century. Furthermore, the movie industry, artists, scientists, and recreationalists have found unique value in BSF, leading to its designation on the U.S. National Register of Historic Places and as an Area of Critical Environmental Concern managed by the Bureau of Land Management.

The objective of this research is to address two fundamental questions that provide insight into the role of anthropogenic and natural processes in driving changes in BSF: (i) how do climatic parameters that influence seasonal flooding, evaporation, and desiccation cycles vary seasonally and over decadal timescales at BSF?; and (ii) how has the footprint of surface halite (*salt crust*) at BSF changed over time? We hypothesize that surface FED cycles are one of the primary drivers of salt crust dissolution and growth and thus will fluctuate on similar timescales. If other drivers, such as regional groundwater hydrology or land use are the primary drivers of change, we would expect to see salt crust changes out of sync with FED cycles. Answering these questions will help to inform understanding of the expected natural variability in the salt crust over annual and decadal timescales that may help to clarify man-made vs. background changes to this dynamic salt playa. In addition, such work will increase our understanding of how sensitive landforms such as playas can be used to constrain and quantify the impacts of accelerated climate and land use changes.

1.1. Regional setting

The Bonneville Salt Flats are located on the northwestern edge of the Bonneville basin within the Great Salt Lake Desert and are bordered by the Silver Island Mountains to the northwest, the Newfoundland basin and Great Salt Lake to the east, and a vast

lacustrine playa to the south (Fig. 1). The elevation of BSF is ~4215 ft. (1284.7 m), which is topographically separated from the adjacent GSL by only ~2 ft. (0.6 m). The GSLD slopes from its low point at BSF up to ~1300 m around its margins. The GSLD is located within the Great Basin in the Basin and Range physiographic province (Fenneman, 1931). The Great Basin is the product of extensional tectonics with normal block faulting and a series of north-south extending mountain ranges separated by low-lying basins with hydrologically closed surface flow but with unknown hydrologic connectivity in the deep subsurface (Gardner and Heilweil, 2014).

The geologic history and formation of BSF is linked to Pleistocene Lake Bonneville and post-Bonneville isostatic rebound (Crittenden, 1963). Lake Bonneville drained after the Last Glacial Maximum and desiccated over the last ~20,000 years. Lake Bonneville had dried to levels similar to current GSL levels by ~13,000 YBP with a brief rise during the Gilbert episode 11,500 YBP that would have reached BSF (Oviatt, 2014). Prior to the Gilbert episode, isostatic rebound elevated the spillway between the GSLD and the Great Salt Lake, effectively isolating the BSF region as a surficially closed, internally draining basin (Oviatt et al., 2015). While past researchers suggested that the GSL may have occasionally flooded the GSLD and may have reached BSF (Eardley, 1962), more recent work suggests that flooding would not have reached BSF at any time through the Holocene (Oviatt, 2015). The saline deposits at BSF are commonly described to be remnants of the final desiccation of Lake Bonneville (White and Terrazas, 2006) but more likely are the result of millions of years of graduate accumulation through large-scale weathering, groundwater flow, and accumulation with groundwater discharge within the GSLD. The presence of subsurface saline deposits from nearby cores suggests that salt was forming in this environment long before the final desiccation of Lake Bonneville (Oviatt et al., 1999). Salt deposits in this area may have experienced many episodes of precipitation and dissolution through geologic time.

1.2. BSF evaporite deposits

The surface dynamics in intracontinental playas are highly sensitive to seasonality of water balance. The saline surface of a salt pan is shaped by surface water and groundwater interactions, with evaporation as the sole output of water (Rosen, 1994; Reynolds et al., 2007). Past work suggested that the general surface morphology and compositional heterogeneity of the BSF region is the result of evaporative zonation, with three incremental concentric stages resulting from sequential saturation of carbonate, gypsum, and halite (Hunt et al., 1966; Lines, 1979). These patterns may generally account for initial deposition of the chemical evaporite sediments in the Bonneville basin, but the current sediment composition (e.g., interbedded eolian gypsum sand and bedded halite) and spatial distribution demonstrate that the surface continues to be modified by continuous eolian processes, erosion, evaporite dissolution, redeposition, subsurface diagenesis, and reworking of the playa.

The surface salt crust at BSF has a general lens-shaped geometry and is composed of up to ~5 ft of interbedded crystalline halite and gypsum sand overlying carbonate muds (White and Terrazas, 2006). The surface morphology of the uppermost halite crust is diverse and dynamic (Fig. 3). At least five distinct halite morphologies have been identified at BSF including thin seasonal salt crust, pressure ridge salt crust, sediment covered salt crust, smooth perennial salt crust, and rough perennial salt crust, all of which are attributed to differing hydrological conditions (Lines, 1979). The timescales of initial salt crust formation and halite crust cycling can be dramatically different in dynamic saline playa environments. For example, Bristol Dry Lake in California has been a playa for the last 10,000 years, yet the oldest sections of halite crust are at most 12 years old (Rosen, 1994). The uppermost halite layer at BSF is of particular interest as it dissolves and reprecipitates annually and provides the hard race track surface that has been prized for over a century by the land speed racing community.

1.3. Human interests in BSF

Since the mid-century, perceptions of a diminishing salt crust have led to concerns among the racing community, questions about best practices for land management, and proposals for mitigation strategies that might lead to additional halite crust formation. Since the mid-century, the BLM has required a study of salt crust volume every 15 years. Past work suggested that the amount of salt at BSF decreased 9–20% in area and 15–31% in volume between 1960 and 1988 (McMillan, 1974; Brooks, 1991). Subsequent research suggested that the volume of the salt crust did not significantly decrease between 1988 and 2003 (White and Terrazas, 2006). While these 15-year snapshots through time provide some insight into possible changes in the overall thickness and volume of the saline deposits at BSF, the decadal timespan between studies does not allow for a direct comparison with changes in climate variables that drive FED cycles. In order to inform decision making about this valued and unique environment, a better understanding is needed of the dynamics that influence the seasonal changes at BSF, and how the extent of the halite crust has changed through time.

Concerns about perceived negative changes in the salt crust led to mitigation efforts beginning in 1997 with the Salt Laydown project (White, 2004). During the winter months, salt from the evaporation ponds south of Interstate 80 is dissolved into a brine that is pumped onto the seasonal surface pond in an effort to increase the thickness and extent of the salt crust. The effectiveness of this process in maintaining or increasing the salt crust is not known. In 2014 and 2015, no racing occurred because of standing water through the summer and because of the lack of reliable and extensive surface halite crust respectively. The changing conditions of BSF are of significant concern to many stakeholder groups including the media, public, government land-use managers, mine operators, and the scientific community. While human activity and interest motivate efforts to understand the changing nature of the BSF, this dynamic setting also provides an opportunity to explore

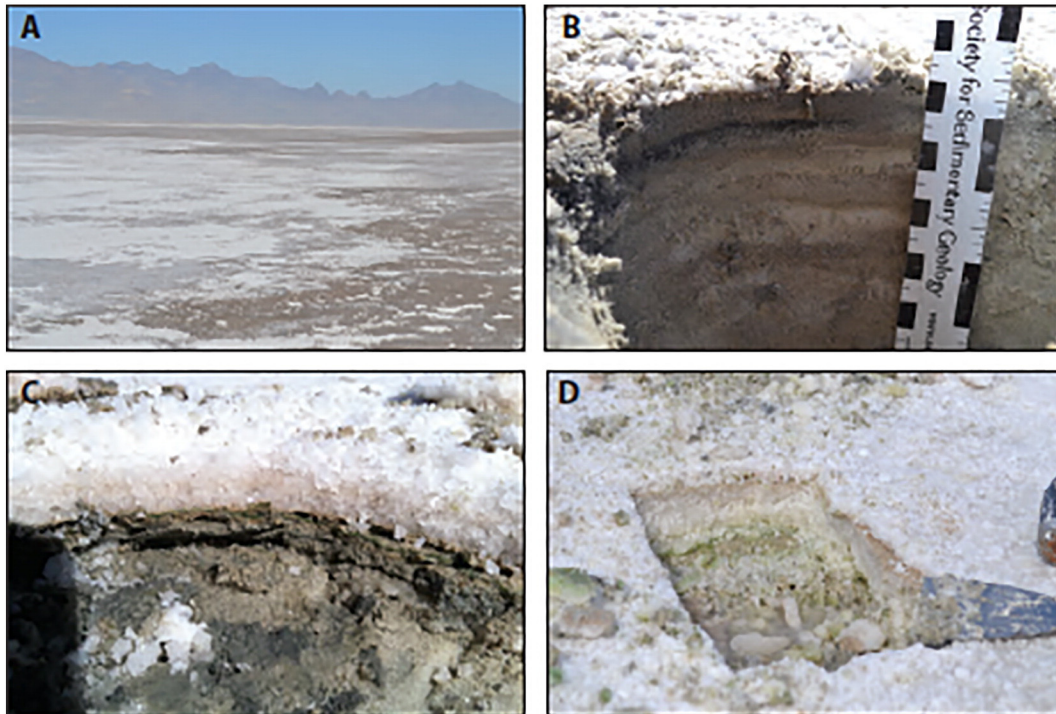


Fig. 3. Examples of BSF salt crust in the field. (A) Photograph of the eastern edge of the halite salt crust showing the diffuse nature of the boundary, October 2015. (B) Excavated pit showing fine-scale stratigraphy of gypsum sand that occurs below the halite crust and just outside the salt crust boundary (note very thin popcorn crust of halite on surface), October 2013. (C) ~4.5 cm-thick surface halite crust overlying organic and clay-rich gypsum sand deposits, October 2013. (D) Example of thicker-bedded halite crust, ~10–15 cm of halite with mm-scale thin beds of clay and pink and green coloration because of the presence of microbes, September 2015.

the natural dynamics and processes of an ephemeral evaporite playa that is closely coupled to local hydrology and climate.

2. Materials and methods

2.1. Climate observations to identify FED cycles

Climate data at BSF was obtained through Mesowest and the National Oceanic and Atmospheric Administration (NOAA) Climate Data Online at the Air Force auxiliary field Wendover, UT, to examine how the seasonality of average water balance parameters (e.g., precipitation and evaporation) change through the year. The Wendover weather station is located ~10 km west-southwest of the southwestern end of BSF (Fig. 1). Mesowest data provide ~20-minute intervals for mean velocity and wind direction from 1997 to the present. NOAA GHCN data provides daily temperatures and precipitation records from 1986 to 2016. Monthly mean temperature values were used to calculate potential evaporation using the Thornthwaite method (Thornthwaite, 1948; Santiago and Vicente-Serrano, 2013). The average annual timing of flooding, evaporation, and desiccation and water balance were evaluated using the Standardized Precipitation Evaporation Index (SPEI) (Vicente-Serrano et al., 2010). The SPEI is an aggregate of precipitation and potential evaporation for a chosen window of time (Fig. 4).

$$SPEI = \frac{P - PET}{\sigma^2} \quad (1)$$

where P = precipitation, PET = potential evapotranspiration, and σ^2 = variance.

2.2. Remote sensing

Landsat satellite scenes were examined from 1986 to 2015 to map the extent of the halite surface salt crust at BSF (Table 1). Annual scenes acquired between August 15 and October 30 with <10% cloud cover were analyzed to map the area of the halite crust at the presumed end of the summer desiccation season. In addition, this time frame was selected for analysis as this is when land speed racing events occur at BSF and when past salt crust thickness studies have been conducted (White and Terrazas, 2006). To map halite, Landsat data were preprocessed to minimize atmospheric signals for analysis of surface reflectance (Young et al., 2017) and spatially subset to focus on the BSF playa area north of I-80 (Fig. 1). In situ spectral data were collected at BSF with an ASD FieldSpec 3 spectroradiometer on 11 June 2014 (Fig. 5). These data were used to calibrate the closest available Landsat scene (from one week prior: 3 June 2014). Surface sediment samples were identified in the field as predominantly halite, gypsum, carbonate, or clay, which have diagnostic textural differences. The mineralogy of these materials was confirmed in the lab using X-ray Diffraction and visible to near-infrared reflectance spectroscopy.

The precise lateral boundary of the surface halite layer can be very difficult to identify in the field because of the diffuse and nonlinear nature of the boundary (Fig. 3). However, spectral analyses allow for an objective and quantifiable definition of the halite surface. Field spectral observations show that the halite crust is characterized by a steep decline in reflectance from 740 to 1500 nm that correspond to a difference between Landsat band 4 (~740 nm) and band 5 (~1500 nm) (Fig. 5). The nonhalite surface facies have spectral signatures with less difference in the overall reflectance at these wavelengths. This difference in spectral reflectance is used to map the halite facies in each scene, where the difference between the reflectance at band 4 is subtracted from the reflectance at band 5, and then normalized to the sum of the reflectance at each band to account for overall changes in albedo.

In order to systematically delineate the area of the halite surface, a threshold value was identified using principal component analysis of

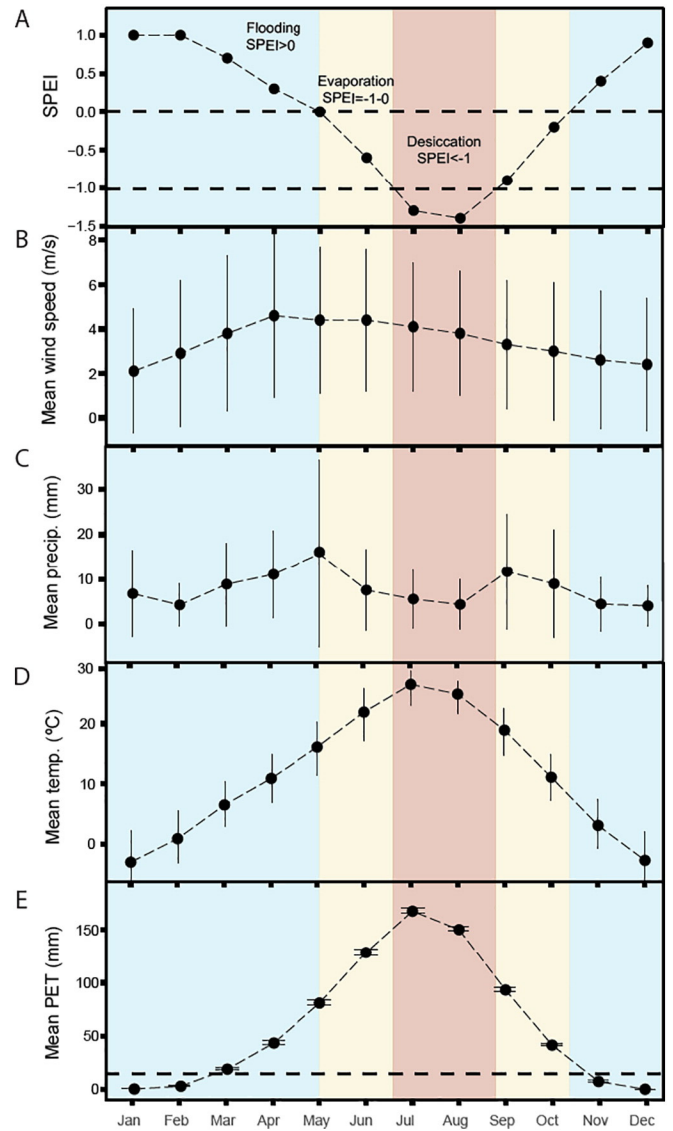


Fig. 4. Mean and standard deviation for monthly climatological variability at BSF from 1985 to 2016 including (A) Standardized Precipitation and Evaporation Index (SPEI), (B) wind speed (wind data available from 1997 to 2016), (C) precipitation, (D) air temperature, and (E) potential evapotranspiration calculated via the Thornthwaite equation. PET exceeds the maximum meteoric water input (~16 mm, dashed line in E) from March to November annually. Month names are shown mid-month. Collectively, these data are used to define annual flooding (blue), evaporation (yellow), and desiccation (orange) cycles.

the greyscale image result of the above-described band index (Fig. 5). A two-dimensional density scatter plot was generated for the first and second Eigenvalues of the principal component scene. This resulted in two density-clusters of pixels, the first correlates with the halite crust and the second with the nonhalite playa boundary. From these results regions of interest were generated on the given band index scenes and for each group statistics were obtained. For 17 scenes, the median eigenvalue for the first percentile of the salt crust was 0.14 and the mean was 0.16. As a reasonable approximation, the eigenvalue 0.155 was then used to delineate the upper threshold for playa boundary and lower threshold for the halite salt crust.

Complications in measurement of area arise when surface water is ponded on top of the halite salt crust. If ponded water did not appear to be directly on the halite crust or appeared to have dissolved the crust, as indicated by low reflectance values for all bands, it was mapped through using the McFeeters (1996) Normalized Difference Water

Table 1

Dates and results of Landsat classification to map halite surface area (date represents when the Landsat scene was collected).

Date (m/d/y)	Area (km ²)
10/28/1986 ^a	139.3
11/29/86	142.6
2/18/1987 ^b	131.0
4/22/87	134.3
6/25/87	162.1
8/12/87	153.9
9/29/87	130.3
10/18/88	119.6
9/2/89	115.4
4/30/90	115.7
6/1/90	129.4
7/3/90	113.2
9/21/90	105.3
10/23/90	102.4
10/10/91	98.0
4/4/92	123.8
5/6/92	117.9
7/25/92	113.1
8/10/92	106.8
9/11/92	106.3
10/13/1992 ^c	100.3
9/29/93	156.2
10/5/95	140.1
10/8/96	102.9
10/26/97	91.3
12/13/1997 ^d	171.2
1/31/1998 ^b	142.2
7/9/98	110.8
9/26/98	117.9
11/2/98	89.8
10/16/99	105.3
9/16/00	121.0
10/5/01	108.1
12/8/2001 ^b	112.9
2/27/2002 ^b	120.8
5/17/02	110.8
7/4/02	105.8
8/5/02	103.8
10/8/02	105.3
10/11/03	93.6
10/13/04	100.4
9/30/05	79.5
10/3/06	110.6
9/30/07	109.7
9/7/08	102.7
9/25/09	96.7
9/29/10	88.2
4/27/11	145.6
7/29/2011 ^b	132.8
8/30/11	123.3
10/17/11	109.5
9/4/13	80.2
10/10/14	72.0
9/10/15	108.2

^a Indicates where a threshold of 0.2 was used.

^b Indicates where supervised maximum likelihood classification was used.

^c Indicates where threshold of 0.1 was used for band index classification.

^d Indicates use of band index classification and analyst selection.

Index (NDWI) and subtracted from the measured area of the halite. Where ponded water was present on and off the crust, a maximum likelihood supervised classification was used to map halite crust with and without water, water not on the crust, and the playa boundary. These results were then used to refine salt crust area maps (see Table 1).

To estimate uncertainty and errors in the classification of halite crust in the Landsat scenes, data collected in June of 2014, were compared with coeval in situ spectral and field data. Confusion matrices were

generated comparing the above band index classification method to in situ ROI and analyst, unsupervised (ISODATA), and supervised classifications (maximum likelihood). The respective methods showed an accuracy of 100, 98, 99, and 96% with a correlated difference in area (compared to band index classification) of 0, 4, 0.5, and 13 km². While our results suggest a reasonable mean uncertainty of 5–6 km², this may vary with environmental conditions on BSF, with a likely increase in uncertainty when ponded water is present.

Halite area was also analyzed over intra-annual timescales ranging from monthly to seasonal time steps during six representative years including 1987, 1998, 1990, 1992, 2002, and 2011 (Figs. 6 and 7). These dates were selected to capture a variety of conditions, including differences in El Nino, reported racing conditions, and differences in land use and management (e.g., salt laydown). In addition, Landsat data over time were qualitatively analyzed to view changes in the local geography of standing water, and precipitation and the relationships between salt crust distribution and wind (Fig. 8).

3. Surface dynamics at the Bonneville Salt Flats

3.1. Defining FED cycles from climate data

Mean monthly climate data for BSF calculated using aggregated daily values from 1985 to 2016 show strong annual seasonal cycles in surface water balance (Fig. 4). Peaks in precipitation occur, on average, during spring and fall. The BSF water balance is positive Nov, Dec, Jan, and Feb and negative the other eight months of the year, thus classifying it as a playa and not a lake (Rosen, 1994). Comparisons to measured pan evaporation in Lines (1979) showed that the Thornthwaite equation for potential evapotranspiration (PET) may underestimate annual evaporation but is deemed as an appropriate approximation during this period of observation given data availability.

To determine typical seasonal FED cycles, Standardized Precipitation and Evaporation Index (SPEI) values were calculated using a two-month moving window. The SPEI has been traditionally used as a tool for determining periods of drought but is used here to examine surface water balance. Flooding seasons are interpreted where the standardized water balance is positive and SPEI is >0 (Fig. 4). Evaporative seasons are identified when the standardized water balance is negative, where SPEI values are between –1.0 and 0. Desiccation is defined as the time period where SPEI values fell below –1.0, when the seasonal standardized water balance is extremely negative.

Using this framework, average periods of flooding occur from the end of October to the middle of May, an evaporation period between mid-May and early July, and desiccation from early July to mid-September. These patterns generally match field observations. One unique result of the climate data analysis is the identification of a second evaporation period following the summer desiccation stage. The BSF experiences two rainy season on average, once in spring and another in fall. These fall periods of rain balanced by higher potential evaporation result in periods of raining and drying between mid-September and late October. The importance of this second period of evaporation in the long-term stability of the salt crust is not known. This time period coincides with the end of annual racing events, when the surface of the salt crust is heavily modified by race track preparation and high vehicular use on the salt.

3.2. Variation in halite salt crust area through time

Measurements of halite salt crust area show significant variance intra-annually and from year to year. Measurements of salt crust area since 1996 show an overall decrease in area through time at a rate of ~12 km² per decade with an R² of 0.3 for the end-summer desiccation stage annual measurements (Fig. 6). The maximum measured annual area was in 1993 with 156.2 km², and the minimum was in 2014 with 71.9 km². The median and mean areas are 102.9 and 106.4 km²

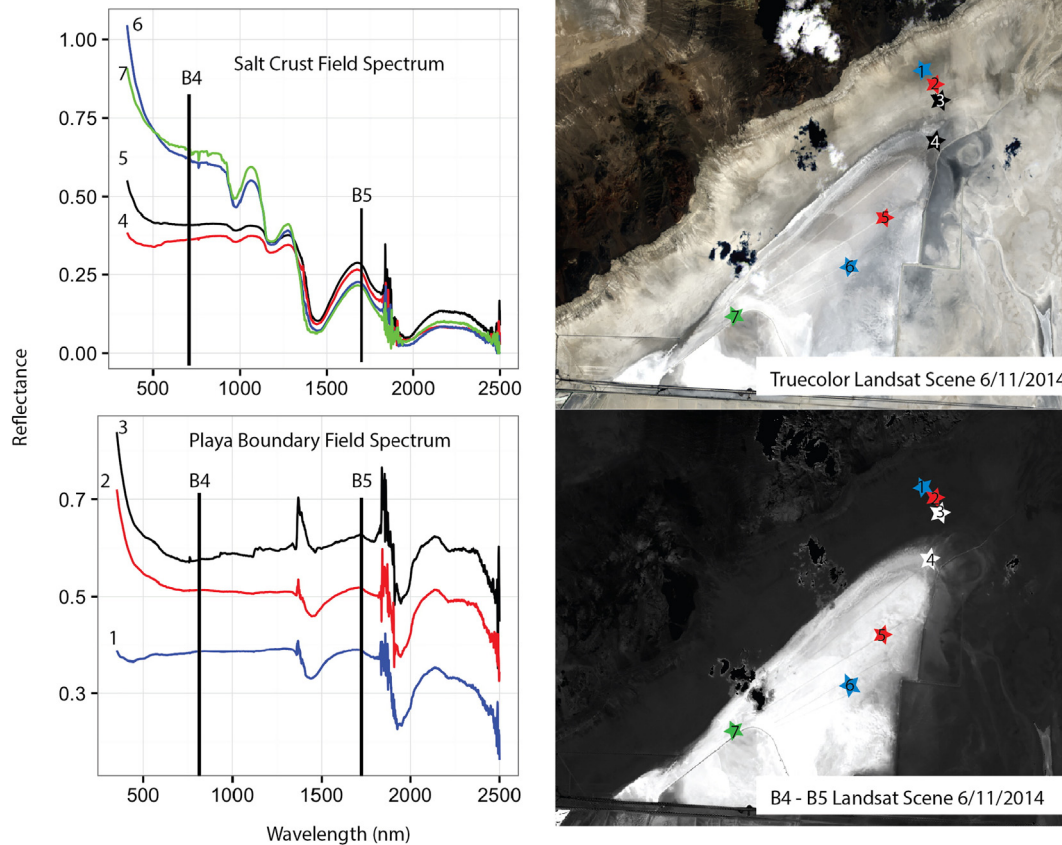


Fig. 5. Visible to near-infrared spectral reflectance signatures of BSF salt crust facies collected in the field on 11 June 2014 (date shown on image as m/d/year). Black vertical bars in plots on left show approximate wavelength locations of band 4 (B4) and band 5 (B5) for Landsat 5. Sites 1–3 are clay- and carbonate-rich playa mud surfaces, while sites 4–7 are on the halite crust. Upper right shows approximate true color Landsat 8 scene obtained 3 June 2014. Lower right gray-scale results from mapping $(\text{band } 5 - \text{band } 6)/(\text{band } 5 + \text{band } 6)$ where band 5 is the near infrared (NIR) at 0.85–0.88 μm and band 6 is in the short wave infrared (SWIR) at 1.57–1.65 μm . Note that Landsat 5 scenes use the designation of bands 4 and 5 for and effectively capture the relationship of $(\text{NIR} - \text{SWIR})/(\text{NIR} + \text{SWIR})$.

respectively. The maximum increase in area in one year was 55.9 km^2 in 1993. The maximum decrease in area for one year was 37.2 km^2 in 1996. The median and mean annual changes in area are -4.5 and -0.8 km^2 respectively. A decrease in salt crust area represents either direct transport of halite out of the system, halite cycling (dissolution and reprecipitation), or extraction of halite-forming solutes through brine withdrawal.

Analysis of the intra-annual variations in halite crust area show considerable variability in the area covered with halite through the year (Fig. 6). Surprisingly, these data show that the end-of-summer desiccation season does not appear to be the season with the greatest aerial coverage of halite (Fig. 7), but rather that area tends to decrease through the year. Recent work on halite precipitation in the Dead Sea has shown that in saline systems that are very close to saturation throughout the year, temperature thresholds for halite precipitation may drive formation of halite from near-saturated brines resulting in halite growth during the winter (Sirota et al., 2016). Seasonal temperature decrease can drive salt formation in the near-saturated brines, which may contribute to the observed intra-annual variations in halite area at BSF where more surface area of halite is observed in the winter months. It is possible that some of the area mapped as salt in the winter could reflect the presence of snow; but the limited footprint analyzed together with field observations of snow typically not accumulating on surfaces saturated with highly saline brine suggests that this is unlikely to be an issue. Bryant (1999) observed that the timing and magnitude of flooding events coinciding with seasonal winds also can play a role in observed annual changes to salt crust surface extent.

3.3. The importance of wind in changing halite footprint

Past work on playa surface dynamics suggests that the interaction of wind, water, and the varying surfaces of a playa significantly alter the morphology and composition of the system (e.g., Wood and Sanford, 1995; Bryant, 1999; Langston and Neuman, 2005; Nield et al., 2014). The role of wind on the redistribution of ponded surface brine has been observed to play a role in salt crust formation, even up slight elevation gradients (Wang et al., 2014). Wind shear over shallow bodies of water (<0.5 m) can result in *roving* lakes that move downwind and potentially uphill where the surface slope of the ponded water responds exponentially to wind speed (Torgersen, 1984). Greater water depths require greater wind speeds in order to equal the same slope gradient achievable at lower speeds and lower depths of ponded water. Such movements have potential to remove water (and salt) from the system without increasing the salinity. The wind-driven patterns in pond location and resulting salt crust area may have additional direct effects on rates of evaporation and salt crust morphology. The effect of surface crust morphology significantly impacts evaporation of the underlying brine. Ponded water tends to produce hard compact surfaces, which subsequently reduces the permeability of a playa substrate and evaporation of groundwater (Groat, 1970). Patchy halite surface morphology can be very conducive to groundwater evaporation, while crusty halite surfaces can decrease evaporation by a factor of 14 (Veran-Tissoires and Prat, 2014).

Wind data from 1997 to 2016 show strong seasonality, with the majority of the wind occurring between spring (March to May) and summer (June to August) and the majority of wind events occurring

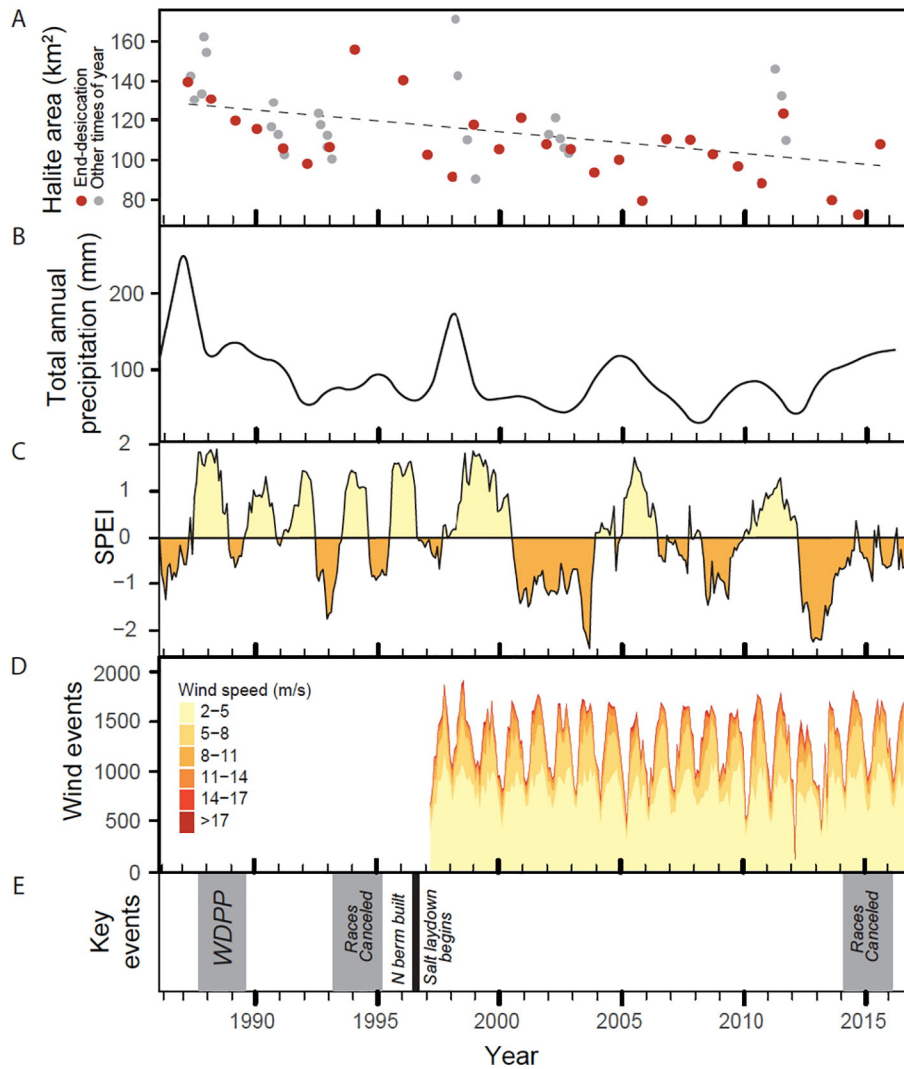


Fig. 6. Time series of observed changes at BSF from 1986 to 2016. (A) Halite salt crust area at BSF measured from Landsat data, (B) total annual precipitation, (C) Standardized Precipitation and Evaporation Index (SPEI) observed over 12-month windows (>0 is wet and <0 is dry), (D) wind events and speed from 1997 (data not available before then), and (E) key human events that have likely played a role in impacting the BSF salt crust.

within these time frames (Fig. 4). The greatest mean wind speeds are recorded in April, with an average of 4.0 m/s. In the spring, speeds are observed >20 m/s, which typically come from the west to northwest and southeast. In the summer season, wind speeds decline with average speeds of ~3.6 m/s and a wind direction from east-southeast. Understanding the effects of wind on the salt crust is complicated as the mechanisms through which it can act are varied and can have opposing effects (e.g., salt loss if brine is blown out of the BSF system and apparent salt gain if salt is spread across a larger area) (Abuduwaili

et al., 2008). In addition, the increased wind may also contribute to increased evaporation. The timing and direction of the wind is important as it occurs in concert with various other parameters such as FED cycles, mining and racing activities, and the Salt Laydown activities in the winter.

The timing and magnitude of individual wind events may play a crucial role in the transport of surface brines and in setting the stage for where salt will form when the surface brine desiccates. Field observations at BSF have shown wind driven surface wave formation resulting in rapid mass movement of the seasonal, dense brine pond. The spreading of this surface pond timed with a decrease in brine temperatures or increasing seasonal evaporation may result in a greater annual halite footprint. The presence of a halite crust can greatly reduce evaporation from the surface pond (Groeneveld et al., 2010; Eloukabi et al., 2013). Future work at BSF will explore the interaction between the surface and subsurface brine with other playa processes (e.g., salt crust formation, eolian transport). Variations in the timing of these weather conditions may result in fluctuation in the area and timing of maximum surface halite extent. Using 2014 as a case study, the wind directions during strong wind events and the geography of the surface water footprint within BSF, correlate with the location and area of surface halite (Fig. 8).

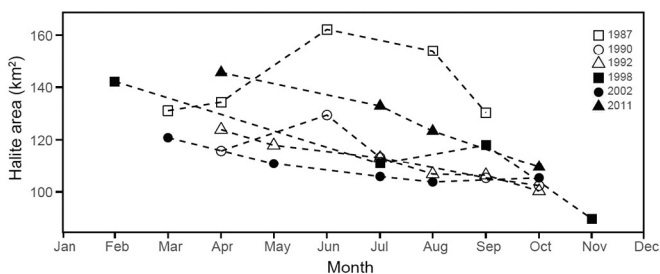


Fig. 7. Intra-annual variations in halite area at BSF calculated from Landsat data during six representative years.

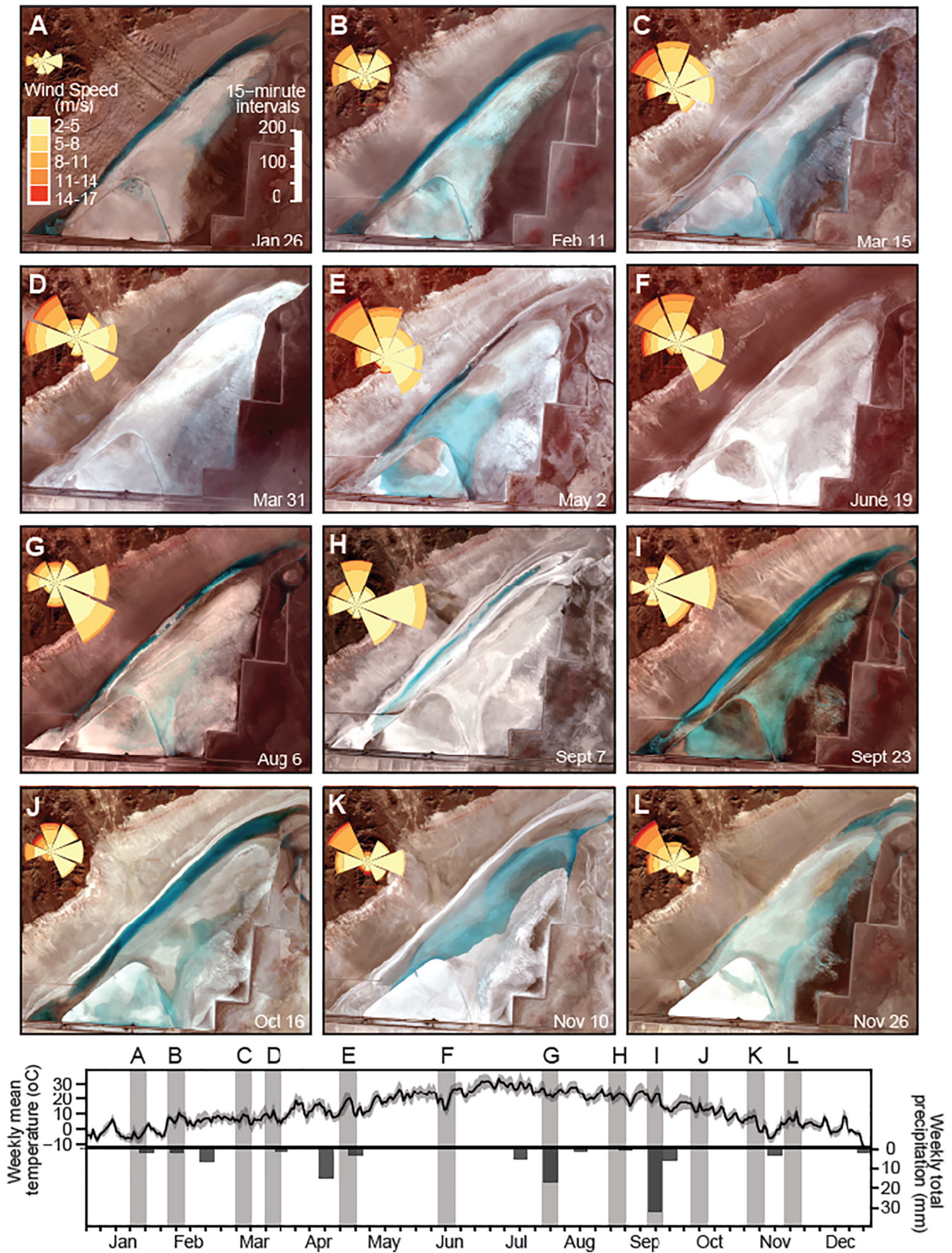


Fig. 8. False color Landsat 8 images (bands 5, 4, and 3 as red, green, and blue respectively) showing the changing footprint of standing water (blues) and halite crust (white) at BSF through 2014 (calendar date on image). Inset wind roses show direction and number of wind events and wind speed for the 2 weeks prior to the image. Note changes in standing water footprint and salt crust with strong winds.

The formation of efflorescent surface salt crust varies with changing evaporation rates of shallow subsurface brine that wicks through the porous media (Eloukabi et al., 2013). In cases where inconsistencies

between the seasonal surface water footprint and surface halite area are observed, efflorescent halite may play a key role in the formation of the surface halite footprint. Further, the flow of water and vapor

through pore space is highly dependent on grain size (Nachshon et al., 2011). Given known heterogeneities in the surface morphology at BSF, the role of efflorescence is likely to be spatially variable.

Mason and Kipp (1998) attributed the estimated redistribution of ~14 million tons of halite in the winter of 1992 to 1993 to the effects of wind and ponded water. Similar to Torgersen (1984), they suggested the potential escape of salt from the system if it happens to be transported beyond subtle yet potential hydrological divides. Lines (1979) described a similar observation of the effects of wind on ponded surface water, noting that the thin seasonal halite crust was largely controlled by surface relief and by the positioning of the surface brine by the wind as it reached its final evaporative stage.

3.4. The role of human activities

Several human processes have likely impacted the area of the salt crust through the three decades analyzed here. In 1987 state authorities began pumping water from the Salt Lake, which had been flooded because of several years of abnormally high precipitation, into the Great Salt Lake Desert just east of BSF (Fig. 6E). The West Desert Pumping Project continued from 1987 to 1989 and had a notable impact on the geochemistry of shallow brines in the West Desert (Kohler, 2002). In 1996, a berm was constructed north of BSF toward Floating Island confining the salt crust as the Salt Laydown Project was initiated, continuing the man-made constraining boundary on the east that is generally formed by the collection ditches (White and Terrazas, 2006). The possible area of the surface pond and salt crust is now limited by mine-related brine collection ditches that bound BSF and I-80 that will block wind-driven pond areas to the east and the south of BSF. This man-made boundary may be one reason that the measured salt crust areas have not reached the levels measured in the mid-1990s (Fig. 6A).

The introduction of additional brine with the wintertime Salt Laydown began in early 1997. The intention of the Salt Laydown has been to specifically remediate the effects of brine withdrawal by contributing more NaCl than is being withdrawn. However, no observed increase in halite occurred with increasing net solutes either in the field or based on this analysis (Fig. 9). The brines introduced to BSF during the Salt Laydown process are only partially saturated, with a brine density of ~1.100 g/mL as compared to a saturation density of 1.204 g/mL at 10 °C (saturation increases with a decrease in temperature). Subsequently, depending on the latency of the Salt Laydown, additional salt crust may actually be dissolved during this process. With the advent of spring, the ponded water is subjected to thinning and areal dispersion from increases in frequency of wind and higher wind speed as well as increases in temperature and evaporation. This may explain why the halite area typically is greater in spring than it is in the fall (Fig. 7).

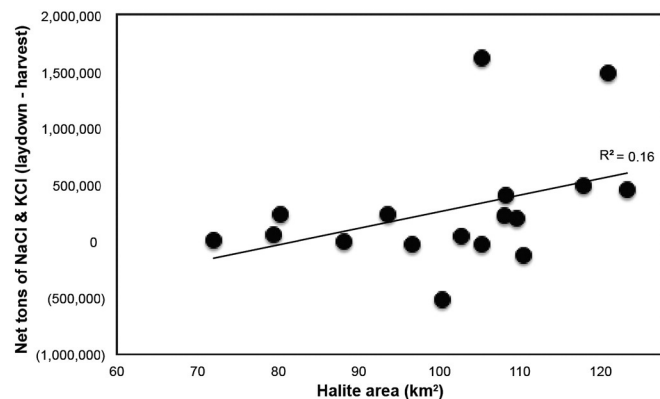


Fig. 9. Comparison of salt crust halite area and net tons of NaCl and KCl cycled via human processes at BSF. Net tonnage includes harvested material and solutes introduced via Salt Laydown from 1998 to 2015.

4. Conclusions

Evaporite playas have been described as one of the most dynamic of landforms with observed variation in surface features on daily, weekly, monthly, and annual scales (Neal and Motts, 1967; Nield et al., 2016). The surface morphology of the Bonneville Salt Flats is actively changing on scales that span from weeks, years, decades, to geological timescales. The surface processes are directly impacted by natural climatic and human events. Our results show that the area of halite salt crust has decreased over the past three decades with significant intra-annual variations. Within the BSF system, the surface salt crust represents only a fraction of the halite within the overall sedimentary package, yet serves as an indicator of system equilibrium. Our analyses do not show a simple relationship between desiccation stage halite area and climate parameters. The area of halite is influenced by the impacts of wind-redistributed ponded brine. Ongoing research will continue to explore the dynamics of the BSF hydrological and biophysical system, the sedimentary and environmental history, and the relationships between this changing ecosystem and the humans that use it. Specifically, future work will examine temporal changes in groundwater brine geochemistry, salt crust thickness, equilibrium exchange between brine and salt crust, as well as local and regional groundwater flow and solute transport.

Acknowledgements

Funding to support this work was provided by NASA EPSCoR RID Grant #NNX13AB34A, NSF Coupled Natural Human Systems Award #1617473, and the University of Utah. We thank reviewers and the editor for detailed feedback that improved the manuscript.

References

- Abuduwaili, J., Gabchenko, M., Junrong, X., 2008. Eolian transport of salts—a case study in the area of Lake Ebinur (Xinjiang, Northwest China). *J. Arid Environ.* 72 (10), 1843–1852.
- Benison, K.C., Bowen, B.B., Oboh-Ikuenobe, F.E., LaClair, D.A., Jagnicki, E.A., Story, S.L., Mormile, M.R., Hong, B.Y., 2007. Sedimentology of acid saline lakes in southern Western Australia: newly described processes and products of an extreme environment. *J. Sediment. Res.* 77, 366–388.
- Bowen, B.B., Benison, K.C., 2009. Geochemical characteristics of naturally acid and alkaline saline lakes in southern Western Australia. *Appl. Geochem.* 24, 268–284.
- Brooks, S.J., 1991. A comparison of salt thicknesses on the Bonneville Salt Flats, Tooele County, Utah during July 1960, October 1974, and October 1988. Bureau of Land Management Technical Memorandum (15 pp).
- Bryant, R.G., 1999. Application of AVHRR to monitoring a climatically sensitive playa. case study: Chott El Djerid, Southern Tunisia. *Earth Surf. Process. Landf.* 24, 283–302.
- Crittenden Jr., M.D., 1963. New Data on the Isostatic Deformation of Lake Bonneville. U.S. Geological Survey on Professional Papers 454–8 (37 pp).
- Eardley, A.J., 1962. Gypsum Dunes and Evaporation History of the Great Salt Lake Desert. Utah Geological and Mineralogy Survey Special Studies 2 (27 pp).
- Eloukabi, H., Sghaier, N., Ben Nasrallah, S., Prat, M., 2013. Experimental study of the effect of sodium chloride on drying of porous media: the crusty-patchy efflorescence transition. *Int. J. Heat Mass Transf.* 56, 80–93.
- Fenneman, N.M., 1931. *Physiography of Western United States*. McGraw-Hill Book, New York.
- Gardner, P.M., Heilweil, V.M., 2014. A multiple-tracer approach to understanding regional groundwater flow in the Snake Valley area of the eastern Great Basin, USA. *Appl. Geochem.* 45, 33–49.
- Groat, C.G., 1970. Geology and hydrology of Troy Playa, San Bernardino County, California. In: Motts, W.S. (Ed.), *Geology and Hydrology of Selected Playas in Western United States*. Massachusetts Univ., pp. 166–199.
- Groeneveld, D.P., Huntington, J.L., Barz, D.D., 2010. Floating brine crusts, reduction of evaporation and possible replacement of fresh water to control dust from Owens Lake bed, California. *J. Hydrol.* 392, 211–218.
- Hunt, C.B., Robinson, T.W., Bowles, W.A., Washburn, A.L., 1966. Hydrologic basin, Death Valley, California. U.S. Geological Survey (Professional Paper 494-B).
- Kohler, J.F., 2002. Effects of the West Desert Pumping Project on the near-surface brines in a portion of the Great Salt Lake Desert, Tooele and Boxelder Counties, Utah. In: Gwynn, J.W. (Ed.), *Great Salt Lake an Overview of Change*.
- Langston, G., Neuman, C.M., 2005. An experimental study on the susceptibility of crusted surfaces to wind erosion: a comparison of the strength properties of biotic and salt crusts. *Geomorphology* 72 (1–4), 40–53.
- Lines, G., 1979. Hydrology and surface morphology of the Bonneville Salt Flats and Pilot Valley playa. Utah. U.S. Bureau of Land Management Report.

- Lowenstein, T.K., Hardie, L.A., 1985. Criteria for the recognition of salt-pan evaporites. *Sedimentology* 32 (5), 627–644.
- Mason, J., Kipp, K., 1998. Hydrology of the Bonneville Salt Flats, Northwestern Utah, and Simulation of Ground-water Flow and Solute Transport in the Shallow-brine Aquifer. U.S. Geological Survey (Professional Paper 1585).
- McFeeters, S.K., 1996. The use of the Normalized Difference Water Index (NDWI) in the delineation of open water features. *Int. J. Remote Sens.* 17 (7), 1425–1432.
- McMillan, D.T., 1974. Bonneville Salt Flats: A comparison of Salt Thickness in July, 1960 and October, 1974: Utah Geological and Mineral Survey Report of Investigation. 91 (6 pp).
- Nachshon, U., Weisbrod, N., Dragila, M.I., Grader, A., 2011. Combined evaporation and salt precipitation in homogeneous and heterogeneous porous media. *Water Resour. Res.* 47 (W03513).
- Neal, J., Motts, W., 1967. Recent geomorphic changes in playas of Western United States. *J. Geol.* 511–525.
- Nield, J.M., Bryant, R.G., Wiggs, G.F., King, J., Thomas, D.S., Eckardt, F.D., Washington, R., 2014. The dynamism of salt crust patterns on playas. *Geology* 43 (1), 31–34.
- Nield, J.M., Wiggs, G.F.S., King, J., Bryant, R.G., Eckardt, F.D., Thomas, D.S.G., Washington, R., 2016. Climate-surface-pore-water interactions on a salt crusted playa: implications for crust pattern and surface roughness development using terrestrial laser scanning. *Earth Surf. Process. Landf.* 41, 738–753.
- Noeth, L.A., 2002. *Bonneville: The Fastest Place on Earth*. MBI Publishing Company, St. Paul, Minnesota.
- Oviatt, C.G., 2014. The Gilbert Episode in the Great Salt Lake Basin, UT. Utah Geological Survey (Miscellaneous Publication 14-3, 20 pp).
- Oviatt, C.G., 2015. Chronology of Lake Bonneville, 30,000 to 10,000 yr B.P. *Quat. Sci. Rev.* 110, 166–171.
- Oviatt, C.G., Thompson, R.S., Kaufman, D.S., Bright, J., Forester, R.M., 1999. Reinterpretation of the Burmester core, Bonneville basin, Utah. *Quat. Res.* 52, 180–184.
- Oviatt, C.G., Madsen, D.B., Miller, D.M., Thompson, R.S., McGeehin, J.P., 2015. Early Holocene Great Salt Lake, USA. *Quat. Res.* 84, 57–68.
- Reynolds, R., Yount, J., Reheis, M., Goldstein, H., Chavez, P., Fulton, R., Forester, R., 2007. Dust emission from wet and dry playas in the Mojave Desert, USA. *Earth Surf. Process. Landf.* 1811–1827.
- Rosen, M., 1994. Importance of groundwater in playas: a review of playa classification and the sedimentology and hydrology of playas. *Geol. Soc. Am. Spec. Pap.*
- Santiago, B., Vicente-Serrano, S.M., 2013. SPEI: Calculation of the Standardized Precipitation-Evapotranspiration Index (R package).
- Sirota, D., Armon, A., Lensky, N.G., 2016. Seasonal variations of halite saturation in the dead sea. *Water Resour. Res.* 52. <https://doi.org/10.1002/2016WR018974>.
- Thorntwaite, C.W., 1948. An approach toward a rational classification of climate. *Geogr. Rev.* 38, 55–94.
- Torgersen, T., 1984. Wind effects on water and salt loss in playa lakes. *J. Hydrol.* 74, 137–149.
- Turk, L., 1973. Hydrogeology of the Bonneville Salt Flats, Utah. Utah Geological and Mineral Survey, Utah Dept. of Natural Resources, Salt Lake City.
- Veran-Tissoires, S., Prat, M., 2014. Evaporation of a sodium chloride solution from a saturated porous medium with efflorescence formation. *J. Fluid Mech.* 749, 701–749.
- Vicente-Serrano, S.M., Beguería, S., López-Moreno, J.I., 2010. A multi-scalar drought index sensitive to global warming: the Standardized Precipitation Evapotranspiration Index – SPEI. *J. Clim.* 23 (DOI: 10.1175/2009JCLI2909.1).
- Wang, J.Z., Cortina, J.L., Kizito, J., 2014. Experimental and theoretical study on temperature distribution of adding coal cinder to bottom of salt gradient solar pond. *Sol. Energy* 110, 756–767.
- Warren, J.K., 2016. *Evaporites: A Geological Compendium*. Springer, USA.
- White, W.W.I.I.I., 2004. Replenishment of salt to the Bonneville Salt Flats: results of the 5-year experimental salt laydown project. *Betting on Industrial Minerals, Proceedings of the 39th Forum on the Geology of Industrial Minerals, 2003*. Nevada Bureau of Mines and Geology, Sparks, Nevada, p. 33 Special Publication.
- White III, W.W., Terrazas, M., 2006. Analysis of Recent and Historical Salt-crust Thickness Measurements and Assessment of Their Relationship to the Salt Laydown Project, Bonneville Salt Flats, Tooele County, Utah.
- Wood, W.W., Sanford, W.E., 1995. Eolian transport, saline lake basins, and groundwater solutes. *Water Resour. Res.* 31 (12), 3121–3129.
- Young, N.E., Anderson, R.S., Chignell, S.M., Vorster, A.G., Lawrence, R., Evangelista, P.H., 2017. A survival guide to Landsat preprocessing. *Ecology* 89 (4), 920–932.